



The Spring-Autumn and Warring States period coldness (400–350 BCE) contributed to the social unrest evidenced from coffin tree rings in southeastern China

Min Zhou^{a,1}, Zhongcai Xiao^{a,1}, Xin Jia^{b,*}, Xuanbo Wang^c, Liangsai Zhu^d, Feifei Zhou^a, Di Zhang^a, Zepeng Mei^a, Mengling Liu^a, Xinyuan Kong^b, Keyan Fang^{a,**}

^a Fujian Institute for Cross-Straits Integrated Development, Key Laboratory of Humid Subtropical Eco-geographical Process (Ministry of Education), Fujian Normal University, Fuzhou, 350007, China

^b Institute of Environmental Archaeology, School of Geography, Nanjing Normal University, Nanjing, 210023, Jiangsu, China

^c Suqian Institute of Cultural Relics Protection and Archaeology, Suqian, 223812, China

^d Lianyungang Institute of Cultural Relics Protection and Archaeology, Lianyungang, 222003, China

ARTICLE INFO

Handling Editor: Dr Yan Zhao

Keywords:

Tree ring
Wooden coffin
Radiocarbon dating
Climate change
Social unrest
Southeastern China

ABSTRACT

China's Spring and Autumn and Warring States period (SAWS, 770–221 BCE) marked the transition from feudal fragmentation to centralized imperial rule. The southeastern region of China, a crucial area for early civilization and socio-economic development, has generally yielded tree-ring paleoclimate records with precise dating shorter than 400 years, thereby limiting research on climatic influences during this epoch. Here, we analyzed coffins unearthed from four archaeological sites dating to the SAWS period in northern Jiangsu, southeastern China. We identified the species as *Phoebe* spp. wood of Lauraceae based on its wood anatomical features. We established four floating chronologies spanning 200–400 years, with radiocarbon dating constraining the temporal ranges to the SAWS period. Our floating chronology represents large-scale temperature variability as indicated by a significantly positive correlation with Northern Hemisphere temperature (NHT) reconstruction. Given the close matches between the floating chronology and NHT, we thus dated the chronology to 492–63 BCE. An anomalous cooling event occurred around 400–350 BCE for the overall warm 492–63 BCE period, coinciding with reduced solar activity. Our study reveals that this cold event may have indirectly triggered frequent large-scale wars and reforms in China's SAWS period. It also coincided with the social unrest in contemporaneous Europe and had widespread impacts. This study provides critical archaeological tree-ring data from a typical monsoon region in China, revealing the significant influence of abrupt climatic events on early society in monsoon regions.

1. Introduction

China's Spring and Autumn and Warring States (SAWS) period (770–221 BCE) marked the transition from feudalism to centralized political governance (Mayhew, 2012; Zhang, 2020). During this period, China experienced a "climatic optimum" in the late Holocene, with warm and humid conditions supporting agricultural expansion and population growth (Liu et al., 2025; Qin et al., 2024; Yin et al., 2021; Zhang et al., 2021a; Zhu, 1972). However, multi-proxy paleoclimatic

records (e.g., tree rings, sediments) revealed some climatic cooling events within this "warm period" (Chen, 2007; Wang et al., 2018; Yin et al., 2021). These cooling events were recurrent occurrences across Eurasian continents (Büntgen et al., 2011; Sigl et al., 2015; Xu et al., 1994; Zhang et al., 2020) and demonstrated temporal correspondence with population migrations (Büntgen et al., 2011) and dynastic transitions (Chen et al., 2019).

As a civilizational nucleus during China's SAWS period (Li et al., 2018), the southeastern region's historical climatic extremes and their

* Corresponding author. Institute of Environmental Archaeology, School of Geography, Nanjing Normal University, Nanjing, 210023, Jiangsu, China.

** Corresponding author. Fujian Institute for Cross-Straits Integrated Development, Key Laboratory of Humid Subtropical Eco-geographical Process (Ministry of Education), Fujian Normal University, Fuzhou, 350007, China.

E-mail addresses: jixin@njnu.edu.cn (X. Jia), kfang@fjnu.edu.cn (K. Fang).

¹ These authors contributed equally to this work.

societal repercussions remain unclear, constrained by the shortness of high-resolution paleoclimate records (Kaufman et al., 2020; Zhang et al., 2021a). While tree-ring records can offer precise and high-resolution dating (Briffa et al., 1990; Cook and Peters, 1997; Fang et al., 2010; Frank et al., 2022; Liu et al., 2025; Qin et al., 2024; Wiles et al., 1996; Xu et al., 2024), existing dendro-chronologies in this region rarely exceed 400 years (Cao et al., 2022; Chen et al., 2012; Zhang et al., 2021b). Notably, the archaeological excavations in northern Jiangsu, southeastern China, unearthed well-preserved Han Dynasty coffins with highly intact tree-ring sequences (Zhu et al., 2022). Based upon species identification and dendro-chronological analysis from those coffins, we establish a 430-year chronology (492–63 BCE) that represents large-scale temperature variability, thereby improving our understanding of the connection between climate change and early societies in southeastern China.

2. Material and methods

2.1. Overview of the study area

The coffin samples were collected from four Han Dynasty tomb sites in Kongwangshan (34.57°N, 119.17°E), Yinmachi (34.57°N, 119.15°E), Jiajiadun (33.72°N, 118.70°E), and Guowang Gaoke (33.68°N, 118.64°E), in northern Jiangsu, southeastern China (Fig. 1a). This region is located in the transition zone between the Huang-Huai Plain and the Jianghuai Plain and is affected by the East Asian monsoon. The annual average temperature is 13–14 °C, and the precipitation is sufficient and concentrated in summer, with long sunshine hours. Characterized by fertile soil, the vegetation exhibits typical transitional features between northern and southern zones, with deciduous broad-leaved forest as the zonal vegetation. Its advantageous geographical location and convenient transportation have historically made it a significant center for economic, cultural, and political activities, leaving behind a wealth of historical remains with substantial archaeological research value.

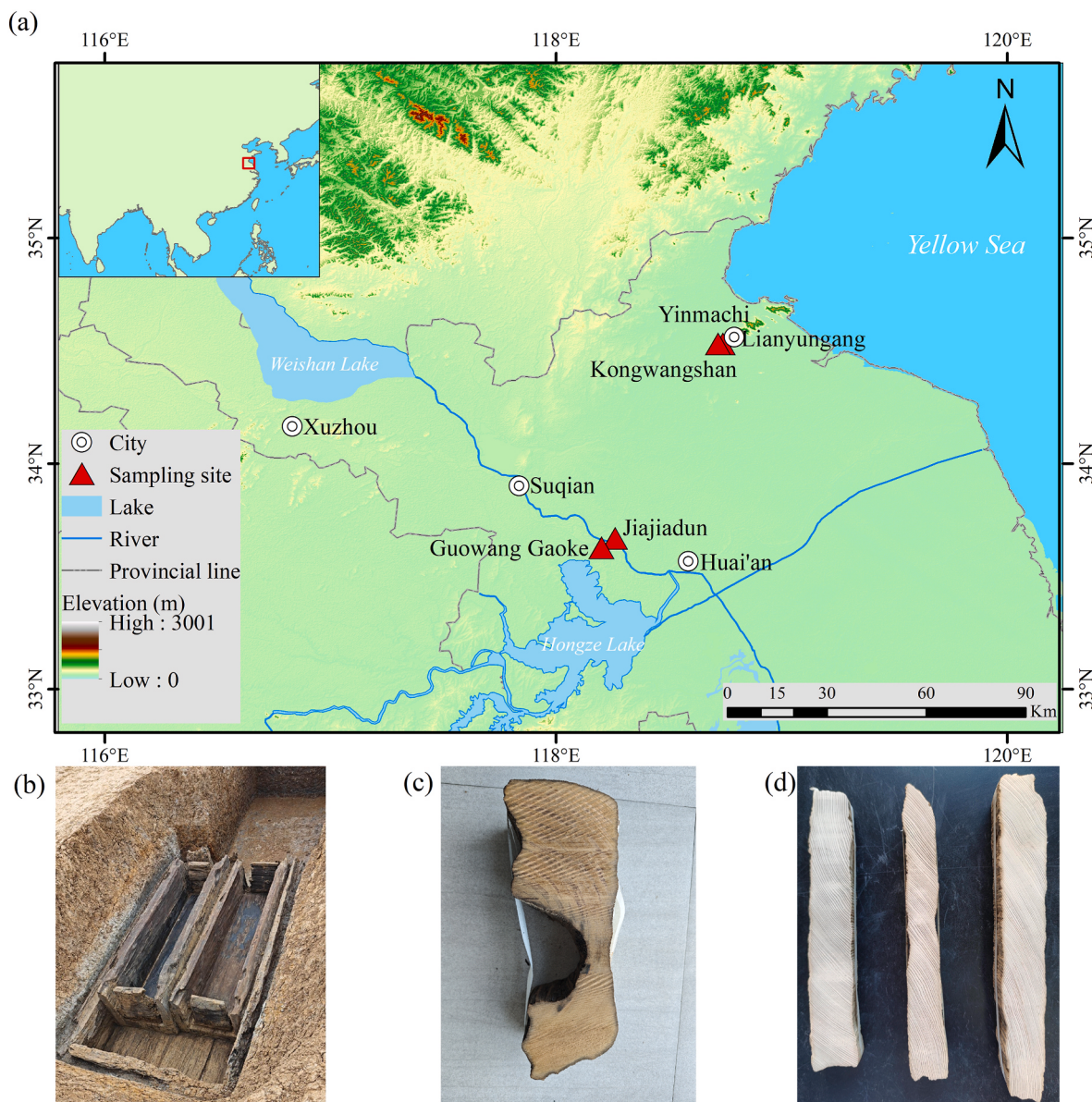


Fig. 1. Overview of the study area. (a) The geographical environment of the study area and the location of sampling sites. (b) Archaeological tomb excavation site, and (c) pictures of coffin wood and (d) polished coffin tree ring samples.

Based on the coffin remains (Fig. 1b) unearthed from the four Han Dynasty tomb sites, 145 well-preserved coffin samples were collected (Table 1). All coffin samples were air-dried and properly stored to ensure quality (Fig. 1c), providing a reliable experimental material foundation for subsequent dendrochronological analysis.

2.2. Tree species identification

To ensure the accuracy and reliability of subsequent dendrochronological analyses, we followed the principle of dendrochronological homogeneity during the wood species identification of the collected coffin samples (Cartwright, 2015; Zhang et al., 2024). Given the antiquity of the coffin samples and their prolonged burial in water-saturated environments (Hoffmann and Jones, 1989), some samples exhibited decay. Consequently, the paraffin embedding and sectioning method was employed to conduct microscopic structural observations, enabling the acquisition of comprehensive wood microstructural characteristics (Zeng, 2000).

The procedure involved: 1) Sample preparation: Small blocks ($1\text{ cm} \times 1\text{ cm} \times 1\text{ cm}$) were cut from the clear tree-ring sections of the coffin wood. Triaxial sections (transverse, radial, tangential) were prepared per sample, with transverse sections encompassing complete rings. The samples were ethanol-glycerol softened (1:1) via boiling, followed by dehydration, clearing, and paraffin infiltration using a KD-BM biological tissue embedding instrument. 2) Paraffin embedding and sectioning: The transverse, radial, and tangential sections were performed using a rotary microtome (KD-2258) with a thickness of $8\text{--}10\text{ }\mu\text{m}$. Paraffin-embedded samples were mounted onto slides and processed through dewaxing, staining, and slide-sealing procedures. 3) Characteristic comparison: Species identification was conducted through systematic analysis of macroscopic anatomical features, supplemented and validated by microscopic examination of wood sections, with parallel comparisons to contemporary reference specimens to ensure taxonomic precision (Gärtner et al., 2015; Von Arx et al., 2016).

2.3. Dendrochronology analysis

The dried coffin wood samples were cut into discs approximately 5 cm thick. Following international dendrochronological standards, the cross-sections of the samples were sequentially ground and polished using sandpapers of 150, 320, 600, 800, and 1500 grit until the annual ring boundaries were visible (Fig. 1d). Subsequently, the ring widths were precisely measured using an LNTAB 5 tree-ring measuring system, with a measurement accuracy of 0.001 mm. Each sample was measured multiple times, and the results were compared to minimize measurement errors. After obtaining the ring width data, precise calendar years were assigned to each ring based on the cross-dating. The COFECHA software was employed to test and correct the cross-dated data (Holmes, 1983). Then, a negative exponential function was fitted using the ARSTAN program to remove the biological trend of tree growth deceleration with age and retain low-frequency signals (Cook and Peters, 1985; Fang et al., 2015). The double-weighted robust mean method was used to integrate the samples, and floating ring-width chronologies for

four archaeological sites were successfully constructed (Gou et al., 2023; Shi et al., 2020). Subsequently, radiocarbon dating was applied to validate this already internally consistent floating chronology and to provide a broad absolute age range for initial calibration. Finally, sliding correlation analysis with the Northern Hemisphere temperature series (Kobashi et al., 2013) was used to achieve precise absolute dating.

2.4. Accelerator mass spectrometry determination of tree-ring ^{14}C age

Coffin wood samples from four Han Dynasty sites were subsampled from middle ring sequences for radiocarbon dating. After surface stabilization, transverse sections (0.5 cm thick) were microtomed and homogenized. α -Cellulose extraction followed the Jayme-Wise chemical procedure (Green, 1963; Kürschner et al., 1962) through sequential treatments: 1) lipid removal with anhydrous ethanol; 2) surface impurities elimination with dilute hydrochloric acid and sodium hydroxide; 3) lignin removal with sodium chlorite and hydrochloric acid; and 4) hemicellulose extraction with 17.5 % sodium hydroxide. Purified cellulose (3.0–4.0 mg) was graphitized and analyzed by MICADAS AMS. Radiocarbon ages were calibrated against IntCal20 using OxCal v4.3.2 (Reimer et al., 2020), reported as “cal yr BP”. The sample pretreatment, graphite target preparation, and dating were all conducted in the ^{14}C Chronology Laboratory at the Key Laboratory of Western China’s Environmental Systems (Ministry of Education), Lanzhou University.

3. Results

3.1. Species identification of coffin wood

From the macroscopic characteristics of the unearthed coffin wood, the surface exhibited a yellowish-brown hue with subtle greenish undertones, presenting a lustrous appearance accompanied by a pronounced aromatic odor. The wood texture was inclined or staggered with a fine-textured structure. The boundaries between earlywood and latewood of annual rings are distinct, and the wood exhibited transitional diffuse to semi-diffuse-porous anatomy, with sparsely distributed vessels of small to medium size (Fig. 2a–c).

Taking the coffin wood from Tomb M135 at the Kongwangshan site as an example, the microscopic features are as follows: the boundary between earlywood and latewood was distinct, with a rapid transition from earlywood to latewood. The vessel elements exhibited circular, oval, and elliptical shapes, with some displaying slightly polygonal outlines, and were uniformly distributed, indicating a diffuse-porous to semi-ring-porous structure. The vessels were arranged in clusters, consisting of solitary vessels and short radial multiples of 2–3 vessels. The vessel diameters ranged between 110 and 170 μm , and tyloses were present within the vessels. The vessel walls exhibited helical thickenings. The axial parenchyma was paratracheal, forming vasicentric bands, and the inter-vessel pits were simple or half-bordered, with circular or oval shapes. The ray tissue was classified as heterogeneous types II and III, and oil cells were present. The wood rays were non-storied, with few uniseriate and multiseriate rays typically 2–3 cells wide and 8–25 cells high (Fig. 2d–f).

Based on the macroscopic and microscopic structural characteristics of the samples provided by literature such as *The Atlas of Gymnosperms Woods of China* (Jiang, 2010) and *The Chinese Timber Chronicle* (Cheng et al., 1992), as well as modern wood microslice calibration, we thus identified the samples as genus *Phoebe* spp.

3.2. Coffin tree-ring chronology and tomb dynasty

A rigorous cross-dating procedure was applied to 145 coffin wood samples. Four floating tree-ring width chronologies were established with periods spanning between 200 and 400 years (Fig. 3). The overall growth trend of the trees was relatively stable, with an average ring width of 1 mm, a minimum width of 0.13 mm, and a maximum width of

Table 1
Information of sampling sites of coffins unearthed from archaeological sites.

Archaeological site	Longitude	Latitude	Sample size	Dynasty
Kongwangshan Site in Lianyungang	119.17°E	34.57°N	10 blocks	Han (202BCE–220CE)
Yinmachi Site in Lianyungang	119.15°E	34.57°N	49 blocks	Western Han (202BCE–8CE)
Jiajiadun Site in Suqian	118.70°E	33.72°N	44 blocks	Han (202BCE–220CE)
Guowang Gaoke Site in Suqian	118.64°E	33.68°N	42 blocks	Han (202BCE–220CE)

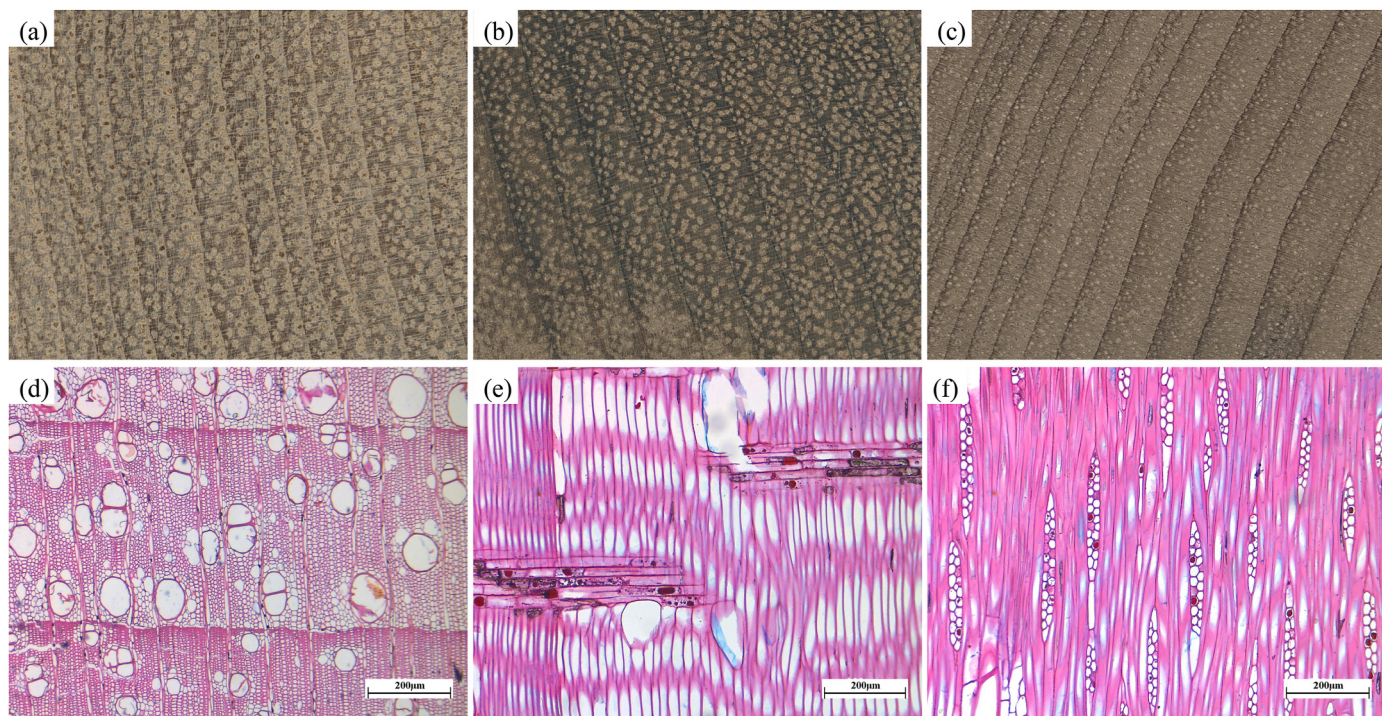


Fig. 2. Macro- and micro-structural characteristics of coffin samples. (a) Kongwangshan M135-4, (b) Yinmachi M38 and (c) Guowang Gaoke M14-6 are the macroscopic characteristics of coffin samples, respectively. (d) Transverse section, (e) radial section and (f) tangential section are the microstructure characteristics of coffin samples, respectively.

2.39 mm. These tree-ring width chronologies are robust according to notable statistical parameters (Table 2). High correlation coefficients indicated a strong consistency in growth trends among the samples. In contrast, high mean sensitivity and signal-to-noise ratios collectively suggested that these chronologies may be climate-sensitive.

To further determine the age information of the coffin, we measured the coffin samples of the precise year by the accelerator mass spectrometer of the ^{14}C years. After the calibration of the tree ring curve IntCal20, under the condition of 95.4 % probability intervals (2σ), the calibrated ages of these chronologies fall roughly between 2500 and 2000 years ago (Table 3 and Fig. 4). However, there are still some error ranges in the dating results. It is noteworthy that both the tomb structures and artifact characteristics provide additional corroborative evidence for dating the ancient burial sites. For example, the vertical earthen-pit tomb M28 at Kongwangshan yielded five-baht coins and green-glazed pottery from the coffin, collectively indicating a late Western Han Dynasty date. In contrast, the vertical stone-chamber tomb M12 at Yinmachi contained glazed ceramics and bronze artifacts attributable to the Western Han period, both further validating the reliability of the dendrochronologically anchored radiocarbon dating results.

3.3. Determination of absolute age

Spatially-representative long-term tree-ring width chronologies still remain underdeveloped in southeastern China due to the relatively short lifespans of extant trees and persistent cross-dating difficulties (Shi et al., 2025a, 2025b). Since evergreen broadleaf trees are sensitive to temperature across southeastern China (Sun, 2003; Wang et al., 2009), the dating of our floating tree-ring chronologies can be improved by a comparison with absolutely dated, annually resolved temperature reconstructions. Consequently, the NHT series was selected due to its dual role as a widely adopted reference standard in paleotemperature studies and demonstrated consistency with published multi-proxy temperature reconstructions over the past two millennia ($r = 0.35\text{--}0.60$, 92–99 %

confidence intervals) (Kobashi et al., 2013).

To further refine the chronological framework, a sliding correlation (sliding step of one year) was analyzed between the four floating tree-ring width chronologies and the reconstructed NHT record over the past 4000 years derived from Greenland ice cores (Kobashi et al., 2013). The significant correlations between them verified that tree growths of *Phoebe* spp. in this region can be a good indicator of large-scale temperature variations. Besides, in combination with the radiocarbon dating of the coffin samples (Table 3), the timespan of the four floating chronologies were ultimately determined (Table 4). The correlations among the four chronologies are relatively weak at interannual timescale (Table S1). However, the Jiajiadun and Kongwangshan chronologies exhibited robust correlations ($P < 0.001$) with the NHT, along with synchronous variations at both high and low-frequency scales (40-year). These results demonstrate stable interannual-to-decadal climatic signals, and thus the chronologies were retained for further analysis (Fig. 5a). Given the synchronized growth variations during their shared period ($n = 94$), we developed a composite chronology with a precise date spanning 492–63 BCE (Fig. 5b), which exhibited stronger temperature correlations than individual series (Table 4). Wavelet coherence analysis confirmed multi-domain phase synchronization between the two records (Fig. 5c and d), validating the chronology's temporal anchoring reliability.

4. Discussion

4.1. Vegetation growth environment and wood source of archaeological sites

When collecting timber resources, humans generally adhere to the “principle of least effort” and the “shortest distance theory” (Shackleton and Prins, 1992). The resource acquisition strategies are closely associated with timber availability. Therefore, the species composition and quantitative characteristics of timber excavating from archaeological sites can provide critical evidence for reconstructing ancient vegetation

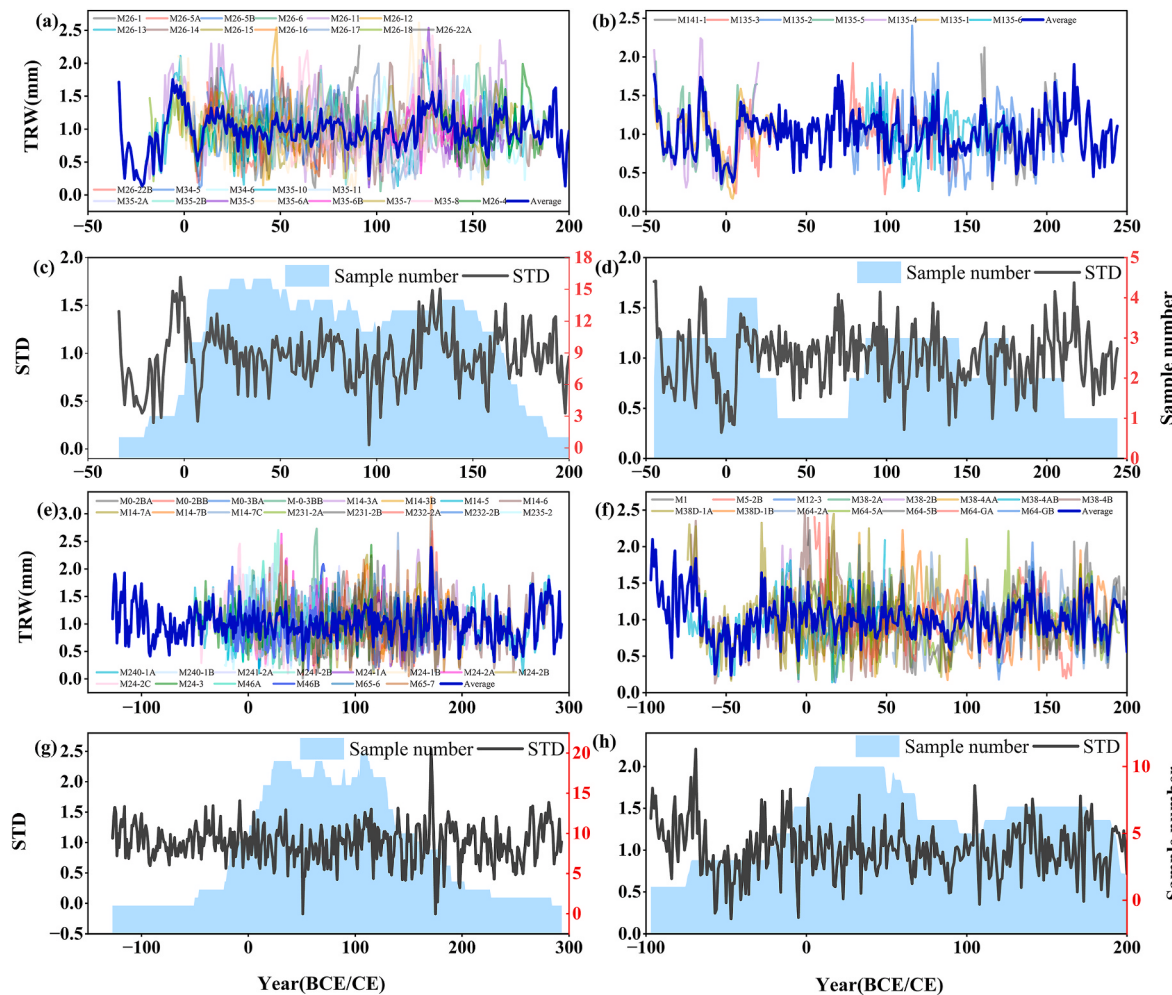


Fig. 3. Tree-ring width sequence, floating chronology, sample size of four archaeological sites. Jiajiadun site (a) 26 tree-ring width sequence comparison and (c) tree-ring floating chronology and sample depth. Kongwangshan site (b) 7 tree-ring width sequence comparison and (d) tree-ring floating chronology and sample depth. Guowang Gaoke site (e) 30 tree-ring width sequence comparison and (g) tree-ring floating chronology and sample depth; Yinmachi site (f) 15 tree-ring width sequence comparison and (h) tree-ring floating chronology and sample depth. The blue bold lines are the average values of all tree-ring width sequences for each site.

Table 2
Statistics on the standard chronology of the width of the coffin tree-ring.

Statistical term	Sampling point			
	Kongwangshan	Yinmachi	Jiajiadun	Guowang gaoke
Sample size	7	15	26	30
Chronological span	290	300	236	421
Standard deviation (SD)	0.093	0.063	0.072	0.041
Average mean sensitivity (MS)	0.328	0.374	0.42	0.39
Inter-sequence correlation (R)	0.505	0.517	0.472	0.519
Signal-to-noise ratio (SNR)	4.698	8.089	5.533	5.518
Expressed population signal (EPS)	0.824	0.89	0.847	0.847

landscapes (Cui et al., 2022). Present study identified the coffin wood as *Phoebe* spp., a species well-known for its exceptional anti-corrosion properties due to its rich content of aromatic oils, tannins, and other natural antimicrobial compounds. This biochemical characteristic made it a preferred material for ancient funerary artifacts (Pan et al., 2013). Archaeological evidence confirms the extensive utilization of *Phoebe* spp. timber (Lauraceae) in mortuary constructions during periods of the

Table 3
Tree-ring radiocarbon dates and calibrated age ranges.

Laboratory number	Sample number	Material	^{14}C age (yr BP)	Calibrated age (cal yr BP)
			2σ (95.4 %)	
LZU24891	Yinmachi M64 GB	α -cellulose	2108 ± 24	2146–1996
LZU24892	Kongwangshan M135-5	α -cellulose	2106 ± 25	2146–1995
LZU24893	Jiajiadun M35-5	α -cellulose	2180 ± 24	2309–2105
LZU24894	Guowang Gaoke M24-3	α -cellulose	2242 ± 24	2335–2155

Pre-Qin (~221BCE) and Han dynasties (202BCE–220CE) (Chen and Chen, 1986; Wu et al., 1985).

Phoebe spp., as a Lauraceous evergreen broad-leaved taxon, currently inhabit in subtropical humid areas such as western Hubei, northwestern Guizhou, and the Sichuan Basin (Lan, 1995; Lin, 1988). However, historical texts and archaeological data indicated significant northward expansion of its historical distributions: the Classic of Mountains and Seas (late Warring States period) records nanmu (*Phoebe zhennan* S. K. Lee & F. N. Wei) growth extending to Shandong and Henan, while the Book of Han account of “There are dense forests in the northern part of the Chu State, where tall trees such as nanmu and camphor trees are

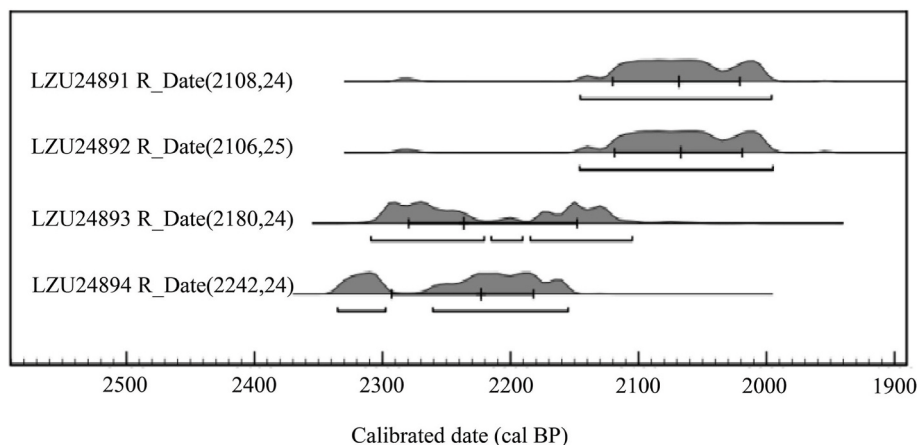


Fig. 4. Calibrated radiocarbon dates from wooden coffins at four archaeological sites. Probability density distributions of four AMS radiocarbon dated coffin wood samples (LZU24891-LZU24894; detailed data in Table 3). Calibration performed using OxCal v4.3.2 and the IntCal20 Northern Hemisphere calibration curve (Reimer et al., 2020). The horizontal axis shows calibrated age in calendar years BP (relative to 1950 CE). Darker shading denotes 95.4 % (2 σ) highest posterior density (HPD) ranges.

Table 4
Sliding correlation results between tree-ring chronologies and NHT series.

Chronology	Time span (BCE)	Correlation coefficient	Time span (BCE)	Correlation coefficient (40-year)
Jiajiadun	492–257	0.219***	492–257	0.493*
Kongwangshan	352–63	0.208***	352–63	0.605
Guowang Gaoke	543–123	0.119*	536–116	0.362
Yinmachi	385–86	0.139*	378–79	0.294
Composite	492–63	0.259***	492–63	0.593**

***, ** and * correspond to the significant levels of 0.001, 0.01 and 0.05, respectively.

grown" (Sima Xiangru's biography) corroborates suitable habitats for *Phoebe* spp. in the Yellow River Basin during the Qin-Han era. This distributional shifts were largely modulated by the Holocene climatic oscillations, characterized by 1–2 °C higher mean annual temperatures than those in modern age (Chen, 2002; Wang, 1995; Zhang and Zhu, 2016; Zhu, 1972). The warming conditions facilitated poleward movement of subtropical vegetations (Jin et al., 2006; Wang et al., 2012).

Notably, the arboreal gigantism of *Phoebe* spp. ("The height of the trunk of nanmu can reach more than ten zhang, and the diameter can reach dozens of circumferences", per the Compendium of Materia Medica) posed logistical challenges for ancient harvesting and transportation. Considering the Pre-Qin woodworking technologies and transport constraints, *Phoebe* spp. timber used for the development of tombs were locally sourced based on the Warring States resource localization strategies documented in the Artificers' Record. However, preferential selection of *Phoebe* spp. wood for its durability may skew paleo-environmental interpretations. Future studies should validate vegetation patterns through comparative analysis of contemporaneous architectural timber assemblages.

4.2. The coffin tree-ring reveals a large-scale climatic cooling anomaly event from 400 to 350 BCE

Although the climate during the SAWS period was generally warm, the narrow tree rings revealed the occurrence of a rapid cold event during 400–350 BCE (Fig. 6a). Such cooling episode have also been corroborated by multiple temperature reconstructions (Büntgen et al., 2011; Kobashi et al., 2013; Shi et al., 2021; Tan et al., 2003; Zhang et al., 2021a). However, notable spatial heterogeneity was observed across different geographical scales (Fig. 6b-f), caused by disparity in the

sensitivity of climate proxies and climate-driven mechanisms. Lines of evidence from historical phenological records and geological archives suggest a coherent cooling signal across southeastern China. For instance, "Mencius: Gaozi I" mentions, "The harvest period of wheat in the middle and lower reaches of the Yellow River in the middle of the Warring States period was around the summer solstice (June 24), which was much later than that in the Spring and Autumn period," reflecting the cold climatic conditions of the time. In addition, the Holocene Jianghan Plain drilling study showed that the proportion of pteridophytes in pollen decreased significantly, and the number of woody plants increased rapidly at about 550 BCE, indicating that the climate was generally cold in this period (Xu et al., 1994). The decrease in the content of warm-type phytoliths recorded by boreholes between 476 and 100 BCE indicated that the climate began to change to cool and humid in the late Warring States period (Tang et al., 1991; Xu et al., 1994), which provides indirect evidence for the low-temperature interpretation of the narrow tree ring event. Although the cold signal was indeed not strong in a minority of sequences, the consistent direction of multiple independent proxies (Table S2) provides convergent evidence supporting the inference of a regional climatic fluctuation during this period. In particular, the temporal consistency between the regional cooling event and the NHT record suggests that this local cooling event may represent a regional manifestation of the coordinated response of the Northern Hemisphere climate system.

4.3. The driving mechanism and spatial synchronization of cooling event

The high consistency observed between the reconstructed sunspot numbers (Solanki et al., 2004), total solar irradiance records (Steinhilber et al., 2012), and the tree-ring width and NHT reconstruction sequences (Kobashi et al., 2013) during the period 400–350 BCE, which suggests that reduced solar activity may have driven temperature declines, thereby limiting tree growth during this interval (Fig. 7a and b, d). The decrease in solar radiation could have enhanced the intensity of the East Asian winter monsoon (e.g., southward expansion of the Siberian High) (Chen et al., 2019) (Fig. 7c), leading to lower temperatures during the growing season and earlier frost occurrences in northern Jiangsu. Anecdotally, tree-ring reconstructions from Central Europe (Büntgen et al., 2011) revealed synchronous cooling features during this period (Fig. 7e), reflecting hemispheric-scale atmospheric circulation reorganization (e.g., southward shift of the westerlies, expansion of the polar vortex). However, the direct radiative effects of solar activity alone cannot fully explain the intensity of the cooling event, necessitating consideration of amplifying feedback mechanisms. For instance, solar

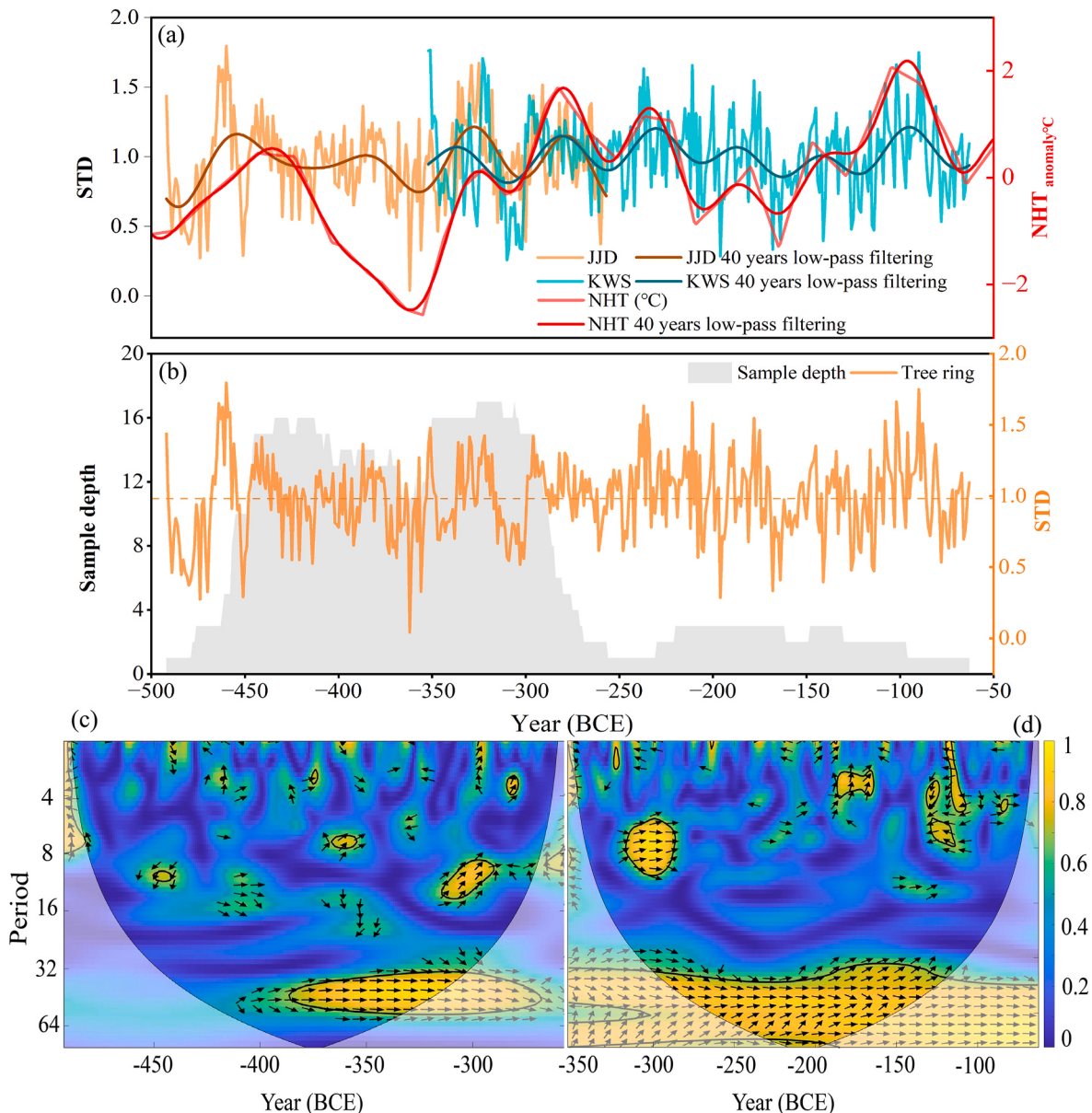


Fig. 5. Absolute dating of coffin tree-ring width floating chronology. (a) The reconstructed NHT (red line) is compared with the established coffin tree-ring width chronologies of Jiajiadun (JJD, yellow line) and Kongwangshan (KWS, blue line). The bold line is the result of a 40-year low-pass filter. (b) Composited tree-ring width sequence and sample depth from this study. The horizontal line represents the average value of the sequence. Cross-wavelet coherence analysis of NHT with (c) Jiajiadun tree-ring width chronology in the range of 492–257 BCE and (d) Kongwangshan tree-ring width chronology in the range of 352–63 BCE.

minima may have prolonged cold periods by triggering increased volcanic activity, resulting in narrow tree rings (Sigl et al., 2015), which requires further validation through tephrochronological data.

4.4. Social unrest of cooling event

Abrupt temperature declines may have triggered crop failures, famines, epidemics (Büntgen et al., 2016; DeMenocal, 2001; Peregrine, 2020; Zonneveld et al., 2024), resource competition (Büntgen et al., 2024; Pederson et al., 2014; Zhang, 2007), and even institutional restructuring (Haldon et al., 2018), potentially leading to the decline and collapse of civilizations (Buckley et al., 2010; Chen et al., 2024a, 2024b; Shen et al., 2024; Zhang et al., 2021c; Zheng et al., 2014).

Climate-driven agricultural crises likely played a pivotal role in this process and potentially accelerated societal transformations. We integrated tree rings with the solar activity and NHT records, and insights from Chinese history studies to establish a link between abrupt climate

change and large-scale social unrest (Fig. 7). During the mid-Warring States period, civil strife, frequent annexation wars and reform movements, such as the Civil Strife of Yue state (375–306 BCE), the Battle of Guiling (354–353 BCE), the Battle of Shaoliang (362 BCE), and the Shangyang Reforms (356/350 BCE) (Fig. 7i), coincided with the timing of climatic cooling. Statistical analysis reveals that the cooling period (400–350 BCE) witnessed an annual average of 1.74 major military campaigns, while concurrently exhibiting a concentration of reforms accounting for approximately 50 % of all reforms throughout the SAWS period (Fig. 7i and Table S3) (Wang, 2007; Zhang et al., 2004). The shortened marching distance represents the weakness of the national strength of the vassal states during this period (Yin et al., 2021) (Fig. 7f). Although precise demographic data are lacking, the scale of battlefield decapitation records (Fig. 7g) and documented epidemic outbreaks (Chen et al., 2022) (Fig. 7h) collectively demonstrated systemic societal vulnerabilities. Cross-regional comparisons highlight the coupling between concurrent hydroclimatic extremes and Qin military food

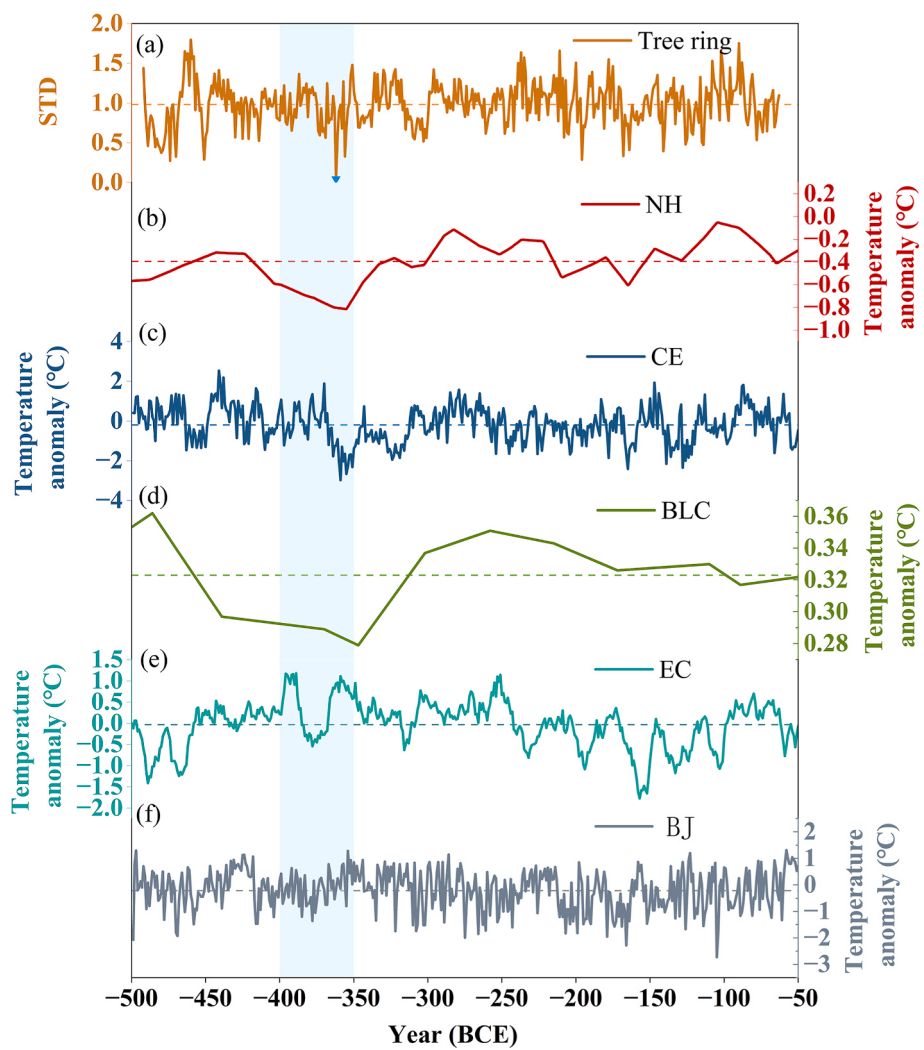


Fig. 6. Comparison of our coffin tree rings and other temperature reconstructions. (a) Composited tree-ring width sequence from this study. (b) The temperature change was reconstructed by the Greenland ice core in the Northern Hemisphere (NH) (Kobashi et al., 2013). (c) The sequence of past 2500 summer temperatures changes in central Europe (CE) (Büntgen et al., 2011). (d) About 30-year resolution and quantitative temperature record based on brGDGTs from Beilianchi (BLC) Lake in northern China (Zhang et al., 2021a). (e) The temperature change was reconstructed by multi-generational indicators in eastern China (EC) (Shi et al., 2021). (f) The temperature change of stalagmite reconstruction in Shihua Cave, Beijing (BJ) (Tan et al., 2003). Each color horizontal line represents the average value of each sequence. Blue shaded areas indicate the cooling period.

shortages during the Battle of Shaoliang (362 BCE) (Liu, 2005; Yao, 2013) (Fig. 7h). This climate change event also triggered social incidents in other regions around the world, the impacts of this cooling event exhibited Eurasian-scale synchronicity-major events such as the southward migration of the Celts (350 BCE) and the Battle of Mantinea (362 BCE) occurred during the cooling period (Büntgen et al., 2011) (Fig. 7e). Although climate cooling is a driving factor rather than a determining factor for social unrest. Our findings suggest that climatic cooling anomaly may have contributed to large-scale frequent war unrest and reform movements during the SAWS period in China, indicating that climatic fluctuations, particularly temperature changes, played a significant role in driving early social transformations.

5. Conclusions

By identifying the species of coffin wood found at archaeological sites in northern Jiangsu, southeast China, this study determined the wood to be *Phoebe* spp. of the Lauraceae. We subsequently constructed a floating tree-ring width chronology by coffins, with radiocarbon dating constraining its temporal range to the SAWS period. The positive correlation between the tree-ring sequence and the NHT reconstruction

dated our tree-ring chronology to 492–63 BCE. The study also found that solar activity may have triggered climatic cooling anomaly events during the SAWS period, which occurred synchronously across Eurasia and coincided with large-scale frequent war unrest and reform movements during the Warring States period in China. Our results revealed the significant influence of abrupt climatic events on early society. The establishment of high-resolution and reliable temperature records in southeastern China will be more conducive to improving the calibration accuracy of the regional tree-ring climate model. Subsequently, the stable carbon/oxygen isotope of the coffin can be extracted to fully extract the hydrological and climatic signals embedded in various dendrochronological parameters and ultimately promote a more robust reconstruction of past climate variability in the region.

Authors contributions

Min Zhou: Conceptualization, Methodology, Formal analysis, Visualization, Writing-original draft, Writing-review & editing; Zhongcai Xiao: Conceptualization, Methodology, Visualization, Writing-original draft, Fieldwork, Resources; Xin Jia: Investigation, Resources, Supervision, Writing-review & editing; Xuanbo Wang: Fieldwork; Liangsai Zhu:

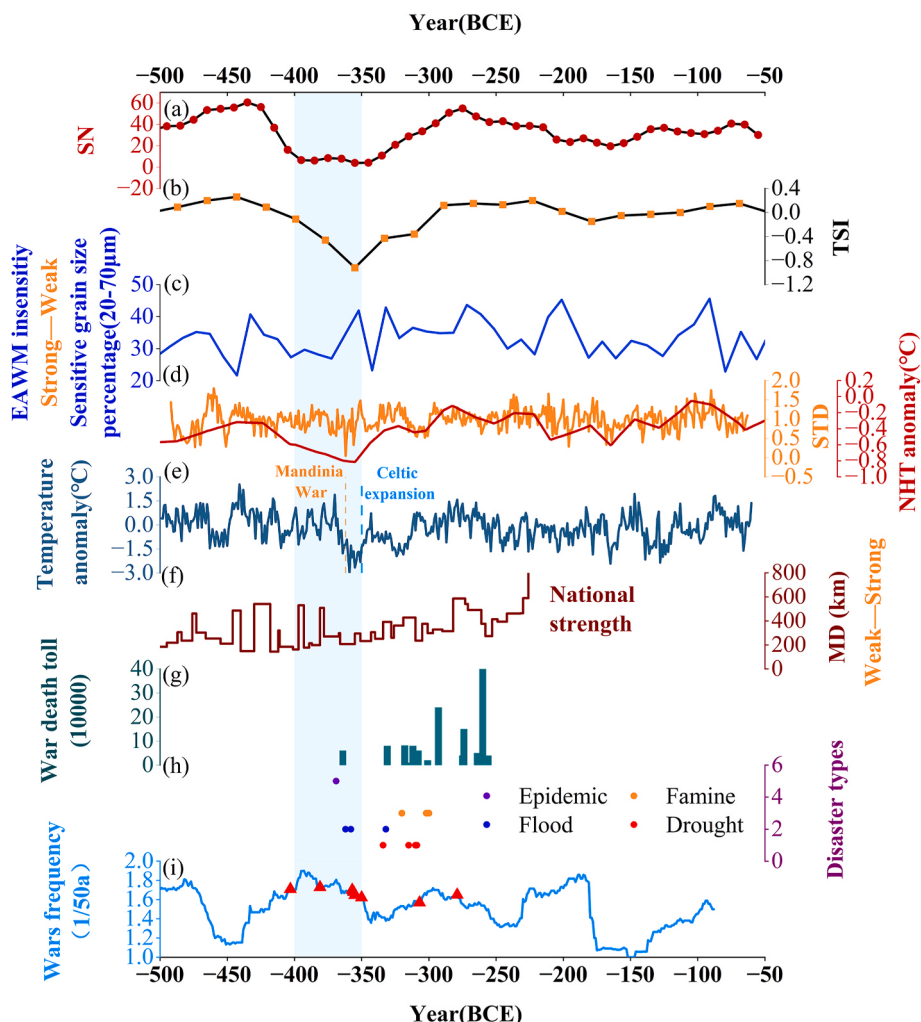


Fig. 7. Climate cooling anomalies and social unrest from the SAWS period. (a) Reconstruction of the sunspot number (SN) (Solanki et al., 2004). (b) Total solar irradiance (TSI) record (Steinhilber et al., 2012). (c) East Asian winter monsoon (EAWM) recorded in sediment in the southern Yellow Sea (Chen et al., 2019). (d) Reconstructed temperature from the Greenland ice core in the Northern Hemisphere (Kobashi et al., 2013) and the tree-ring width sequence from this study. The thickening line is the result of 40 years of low-pass filtering. (e) The sequence of past 2500 summer temperatures changes in central Europe (Büntgen et al., 2011). (f) Annual average marching distance (MD) in the SAWS period is calculated quantitatively based on historical literature records (Chen et al., 2022). (g) Historical records of the number of beheading and captives in wars during the Warring States period (Zhang, 2007). (h) Disasters, famines, and epidemics record from the SAWS period in historical documents (Chen et al., 2022; Liu, 2005; Yao, 2013). (i) The frequency of wars every 50 years is based on the original statistical chronology of wars in Chinese history. Major reforms during the SAWS period are marked by a red triangle (Yin et al., 2021). Blue shaded areas indicate the cooling period.

Fieldwork; Feifei Zhou: Conceptualization, Methodology, Formal analysis, Fieldwork, Writing-review & editing; Di Zhang: Fieldwork, Formal analysis; Methodology, Investigation; Zepeng Mei: Fieldwork, Investigation; Mengling Liu: Fieldwork, Investigation; Xinyuan Kong: Fieldwork; Keyan Fang: Conceptualization, Funding acquisition, Methodology, Resources, Supervision, Validation, Writing-review & editing.

Declaration of competing interest

The authors declare that they have no known competing financial interests or personal relationships that could have appeared to influence the work reported in this paper.

Acknowledgements

This study was supported by the National Natural Science Foundation of China (42425101, 41988101, and 42301058), and Fujian Institute for Cross-Straits Integrated Development (LARH24JBO7).

Appendix A. Supplementary data

Supplementary data to this article can be found online at <https://doi.org/10.1016/j.quascirev.2025.109617>.

Data availability

All data and/or code is contained within the submission.

References

- Briffa, K.R., Bartholin, T.S., Eckstein, D., Jones, P.D., Karlén, W., Schweingruber, F.H., Zetterberg, P., 1990. A 1,400-year tree-ring record of summer temperatures in Fennoscandia. *Nature* 346, 434–439. <https://doi.org/10.1038/346434a0>.
- Buckley, B.M., Anchukaitis, K.J., Penny, D., Fletcher, R., Cook, E.R., Sano, M., et al., 2010. Climate as a contributing factor in the demise of Angkor, Cambodia. *Proc. Natl. Acad. Sci. USA* 107, 6748–6752. <https://doi.org/10.1073/pnas.0910827107>.
- Büntgen, U., Eggertsson, O., Oppenheimer, C., 2024. Braided motivations for Iceland's first wave of mass emigration to North America after the 1875 Askja eruption. *Reg. Environ. Change* 24, 48. <https://doi.org/10.1007/s10113-024-02215-6>.
- Büntgen, U., Myglan, V.S., Ljungqvist, F.C., McCormick, M., Di Cosmo, N., Sigl, M., et al., 2016. Cooling and societal change during the Late Antique Little Ice Age from 536 to around 660 AD. *Nat. Geosci.* 9, 231–236. <https://doi.org/10.1038/ngeo2652>.

- Büntgen, U., Tegel, W., Nicolussi, K., McCormick, M., Frank, D., Trouet, V., et al., 2011. 2500 years of European climate variability and human susceptibility. *Science* 331, 578–582. <https://doi.org/10.1126/science.1197175>.
- Cao, X.G., Hu, H.B., Kao, P.-k., Buckley, B.M., Dong, Z.P., Chen, X.L., et al., 2022. Improved spring temperature reconstruction using earlywood blue intensity in southeastern China. *Int. J. Climatol.* 42, 6204–6220. <https://doi.org/10.1002/joc.7585>.
- Cartwright, C.R., 2015. The principles, procedures and pitfalls in identifying archaeological and historical wood samples. *Ann. Bot.* 116, 1–13. <https://doi.org/10.1093/aob/mcv056>.
- Chen, C.Z., Zhao, W.W., Xia, Y.X., Gu, Q.R., Li, H., Cao, X.Y., et al., 2024b. Holocene climatic transition in the Yangtze River region and its impact on prehistoric civilizations. *Catena* 238, 107886. <https://doi.org/10.1016/j.catena.2024.107886>.
- Chen, F., Yuan, Y.J., Wei, W.S., Yu, S.L., Zhang, T.W., 2012. Tree ring-based winter temperature reconstruction for Changting, Fujian, subtropical region of Southeast China, since 1850: linkages to the Pacific Ocean. *Theor. Appl. Climatol.* 109, 141–151. <https://doi.org/10.1007/s00704-011-0563-0>.
- Chen, G.H., Zhou, X.Y., Khasanov, M., Ma, J., Liu, J.C., Shen, H., et al., 2024a. Oasis civilization collapse under 3.9 ka climate event in Bactria, Central Asia. *Quat. Sci. Rev.* 337, 108793. <https://doi.org/10.1016/j.quascirev.2024.108793>.
- Chen, J., Chen, L.H., 1986. Summary of cleaning the tomb of Southern song dynasty in Wujin Village, Jiangsu Province. *Archaeol. Ocean.* 3, 247–260+268+295–296.
- Chen, J.X., Nan, Q.Y., Li, T.G., Sun, R.T., Sun, H.J., Lu, J., 2019. Variations in the East Asian winter monsoon from 3500 to 1300 cal. yr BP in northern China and their possible societal impacts. *J. Asian Earth Sci.* 181, 103912. <https://doi.org/10.1016/j.jseas.2019.103912>.
- Chen, S., Wei, Y., Yue, X.A., Xu, K.H., Li, M.K., Lin, W., 2022. Correlation analysis between the occurrence of epidemic in ancient China and solar activity. *Sci. China Earth Sci.* 66, 1–8. <https://doi.org/10.1007/s11430-022-9986-5>.
- Chen, Y.X., 2002. A historical Re-investigation of climatic conditions during the west and East Han dynasties. *Hist. Res.* 4, 76–95 + 190.
- Chen, Y.X., 2007. A study on the climate in the area of the middle of Yangtze River from the Zhanguo period to the East Han dynasty. *J. Chin. Hist. Geogr.* 22, 5–16. <https://doi.org/10.3969/j.issn.1001-5205.2007.01.001>.
- Cheng, J.Q., Yang, J.J., Liu, P., 1992. *Chinese Timber Chronicle*. China Forestry Publishing House, Beijing.
- Cook, E.R., Peters, K., 1985. A Time Series Analysis Approach to Tree Ring Standardization (Dendrochronology, Forestry, Dendroclimatology, Autoregressive Process). The University of Arizona, Arizona.
- Cook, E.R., Peters, K., 1997. Calculating unbiased tree-ring indices for the study of climatic and environmental change. *Holocene* 7, 361–370.
- Cui, H.Q., Wang, S.Z., Zhang, X.H., Jin, H.T., Jiao, Y.J., Xia, Z.K., 2022. The ecological environment and wood utilization indicated by the charcoal remains of the Bronze Age site in Minhe County, Guanting basin, Qinghai Province. *Quat. Sci.* 42, 158–171. <https://doi.org/10.11928/j.issn.1001-7410.2022.01.13>.
- DeMenocal, P.B., 2001. Cultural responses to climate change during the late Holocene. *Science* 292, 667–673. <https://doi.org/10.1126/science.1059287>.
- Fang, K.Y., Gou, X.H., Chen, F.H., Li, J.B., D'Arrigo, R., Cook, E., et al., 2010. Reconstructed droughts for the southeastern Tibetan Plateau over the past 568 years and its linkages to the Pacific and Atlantic Ocean climate variability. *Clim. Dyn.* 35, 577–585. <https://doi.org/10.1007/s00382-009-0636-2>.
- Fang, K.Y., Yang, B., Zheng, H.Z., Li, Y.J., Zhou, F.F., Dong, Z.P., et al., 2015. Applying tree-ring methods in the global changes studies. *Quat. Sci.* 35, 1283–1293. <https://doi.org/10.11928/j.issn.1001-7410.2015.05.24>.
- Frank, D., Fang, K.Y., Fonti, P., 2022. Dendrochronology: fundamentals and innovations. In: *Stable Isotopes in Tree Rings: Inferring Physiological, Climatic and Environmental Responses*. Springer International Publishing, pp. 21–59. https://doi.org/10.1007/978-3-030-92698-4_2.
- Gärtner, H., Banzer, L., Schneider, L., Schweingruber, F.H., Bast, A., 2015. Preparing micro sections of entire (dry) conifer increment cores for wood anatomical time-series analyses. *Dendrochronologia* 34, 19–23. <https://doi.org/10.1016/j.dendro.2015.03.004>.
- Gou, X.X., Zhang, T.W., Yu, S.L., Liu, K.X., Zhang, R.B., Shang, H.M., et al., 2023. Climate response of *Picea schrenkiana* based on tree-ring width and maximum density. *Dendrochronologia* 78, 126067. <https://doi.org/10.1016/j.dendro.2023.126067>.
- Green, J.W., 1963. *Wood Cellulose, Methods in Carbohydrate Chem Istry*. Academic Press, New York, pp. 9–21.
- Haldon, J., Elton, H., Huebner, S.R., Izdebski, A., Mordechai, L., Newfield, T.P., 2018. Plagues, climate change, and the end of an empire: a response to Kyle Harper's The Fate of Rome (I): climate. *Hist. Compass* 16, e12508. <https://doi.org/10.1111/hic.12508>.
- Hoffmann, P., Jones, M.A., 1989. Structure and degradation process for waterlogged archaeological wood, archaeological wood. *Am. Chem. Soc.* 35–65. <https://doi.org/10.1021/ba-1990-0225.ch002>.
- Holmes, R.L., 1983. Computer-assisted quality control in tree-ring dating and measurement. *Tree-Ring Bull.* 43, 51–67. <http://hdl.handle.net/10150/261223>.
- Jiang, X.M., 2010. *Atlas of Gymnosperms Woods of China*. Science Press, Beijing.
- Jin, G.Y., Yu, H.G., Luan, F.S., Wang, C.Y., Undermill, A.P., Yao, X.S., 2006. Climate significance of wood samples from Liangchengzhen Longshan culture site (4600~4000 a.B.P.), Rizhao, Shandong. *Quat. Sci.* 4, 571–579.
- Kaufman, D., McKay, N., Routson, C., Erb, M., Davis, B., Heiri, O., et al., 2020. A global database of Holocene paleotemperature records. *Sci. Data* 7, 115. <https://doi.org/10.1038/s41597-020-0445-3>.
- Kobashi, T., Goto-Azuma, K., Box, J.E., Gao, C.C., Nakaegawa, T., 2013. Causes of Greenland temperature variability over the past 4000 yr: implications for northern hemispheric temperature changes. *Clim. Past* 9, 2299–2317. <https://doi.org/10.5194/cp-9-2299-2013>.
- Kürschner, K., Popik, M.G., Kürschner, K., Popik, M.G., 1962. Zur Analyse von Hölzern. *Holzforschung* 16, 1–11. <https://doi.org/10.1515/hfsg.1962.16.1.1>.
- Lan, Y., 1995. Study on the changes of geographical distribution of *Phoebe* nees in historical period. *J. Chin. Hist. Geogr.* 19–32.
- Li, J.Y., Dodson, J., Yan, H., Wang, W.M., Innes, J.B., Zong, Y.Q., et al., 2018. Quantitative Holocene climatic reconstructions for the lower Yangtze region of China. *Clim. Dyn.* 50, 1101–1113. <https://doi.org/10.1007/s00382-017-3664-3>.
- Lin, H.G., 1988. Ancient nanmu and its distribution changes. *J. Sichuan Forest. Sci. Technol.* 4, 48–58.
- Liu, J.G., 2005. Review of Pre-Qin Disasters. *Zhengzhou University*.
- Liu, Y., Song, H.M., An, Z.S., Li, Q., Leavitt, S.W., Büntgen, U., et al., 2025. Recent centennial drought on the Tibetan Plateau is outstanding within the past 3500 years. *Nat. Commun.* 16, 1311. <https://doi.org/10.1038/s41467-025-56687-z>.
- Mayhew, G.L., 2012. The formation of the Qin dynasty: a socio-technical system of systems. *Procedia. Comput. Sci.* 8, 402–412. <https://doi.org/10.1016/j.procs.2012.01.079>.
- Pan, B., Zhai, S.C., Fan, C.S., 2013. Wood identification and properties analysis of the coffin timbers taken from Lizhouao ancient tomb in Jiang'an county of Jiangxi. *J. Nanjing Forestry Univ. (Natural Sciences Edition)* 37, 87–91. [https://doi.org/10.1000-2006\(2013\)03-0087-05](https://doi.org/10.1000-2006(2013)03-0087-05).
- Pederson, N., Hessl, A.E., Baatarbileg, N., Anchukaitis, K.J., Cosmo, N.D., Pederson, N., et al., 2014. Pluvials, droughts, the Mongol Empire, and modern Mongolia. *Proc. Natl. Acad. Sci. USA.* 111, 4375–4379. <https://doi.org/10.1073/pnas.1318677111>.
- Peregrine, P.N., 2020. Climate and social change at the start of the Late Antique Little Ice Age. *Holocene* 30, 1643–1648. <https://doi.org/10.1177/0959683620941079>.
- Qin, C., Yang, B., Bräuning, A., Charpentier, Ljungqvist, F., Osborn, T.J., Shishov, V., et al., 2024. Persistent humid climate favored the Qin and Western Han Dynasties in China around 2,200 y ago. *Proc. Natl. Acad. Sci. USA.* 122, e2415294121. <https://doi.org/10.1073/pnas.2415294121>.
- Reimer, P.J., Austin, W.E.N., Bard, E., Bayliss, A., Blackwell, P.G., Ramsey, C.B., et al., 2020. The IntCal20 Northern Hemisphere radiocarbon age calibration curve (0–55 cal kBP). *Radiocarbon* 62, 725–757. <https://doi.org/10.1017/RDC.2020.41>.
- Shackleton, C.M., Prins, F., 1992. Charcoal analysis and the "principle of least effort"-a conceptual model. *J. Archaeol. Sci.* 19, 631–637. [https://doi.org/10.1016/030-4403\(92\)90033-Y](https://doi.org/10.1016/030-4403(92)90033-Y).
- Shen, C.C., Beardsley, F., Gong, S.Y., Kataoka, O., Yoneda, M., Yokoyama, Y., et al., 2024. Links between climatic histories and the rise and fall of a Pacific chiefdom. *PNAS Nexus* 3, 399. <https://doi.org/10.1093/pnasnexus/pgac399>.
- Shi, F., Lu, H.Y., Guo, Z.T., Yin, Q.Z., Wu, H.B., Xu, C.X., et al., 2021. The position of the current warm period in the context of the past 22,000 years of summer climate in China. *Geophys. Res. Lett.* 48, e2020GL091940. <https://doi.org/10.1029/2020GL091940>.
- Shi, F., Yang, B., Linderholm, H.W., Seftigen, K., Yang, F.M., Yin, Q.Z., et al., 2020. Ensemble standardization constraints on the influence of the tree growth trends in dendroclimatology. *Clim. Dyn.* 54, 3387–3404. <https://doi.org/10.1007/s00382-020-05179-5>.
- Shi, S.Y., Shi, J.F., Nakatsuka, T., Sano, M., Li, Z., Shu, J.P., et al., 2025b. Tree-ring oxygen isotope cross-dating between southeastern China and central Japan. *Dendrochronologia* 91, 126319. <https://doi.org/10.1016/j.dendro.2025.126319>.
- Shi, S.Y., Xiao, C.C., Li, Z.B., Wang, Y.X., Wang, H., Niu, Z.S., et al., 2025a. Tree-ring dating of the construction of the Yinshan tomb in Shaoxing, Zhejiang Province: a preliminary study. *Sci. China. Earth. Sci.* 68, 1960–1973. <https://doi.org/10.1007/s11430-024-1572-5>.
- Sigl, M., Winstrup, M., McConnell, J.R., Welten, K.C., Plunkett, G., Ludlow, F., et al., 2015. Timing and climate forcing of volcanic eruptions for the past 2,500 years. *Nature* 523, 543–549. <https://doi.org/10.1038/nature14565>.
- Solanki, S.K., Usoskin, I.G., Kromer, B., Schüssler, M., Beer, J., 2004. Unusual activity of the Sun during recent decades compared to the previous 11,000 years. *Nature* 431, 1084–1087. <https://doi.org/10.1038/nature02995>.
- Steinhilber, F., Abreu, J.A., Beer, J., Brunner, I., Christl, M., Fischer, H., et al., 2012. 9,400 years of cosmic radiation and solar activity from ice cores and tree rings. *Proc. Natl. Acad. Sci. USA.* 109, 5967–5971. <https://doi.org/10.1073/pnas.1118965109>.
- Sun, Y., 2003. Study on the Relationship Between Carbon Isotope and Climate Change in Ancient Trees and Modern Tree Rings in South China. Peking University, Beijing.
- Tan, M., Liu, T.S., Hou, J.Z., Qin, X.G., Zhang, H.C., Li, T.Y., 2003. Cyclic rapid warming on centennial-scale revealed by a 2650-year stalagmite record of warm season temperature. *Geophys. Res. Lett.* 30, 1617. <https://doi.org/10.1029/2003GL017352>.
- Tang, L.Y., Shen, C.M., Han, H.Y., Yu, G., Xiao, J.Y., 1991. Preliminary study on the 7500–5000aB.P. climatic change sequence in the middle and lower reaches of the Yangtze River. *Mar. Geol. Quat. Geol.* 73–85. <https://doi.org/10.16562/j.cnki.0256-1492.1991.04.010>.
- Wang, B., Gao, P., Guo, H., Leng, L., 2009. Responses of tree-ring width of *Cinnamomum camphora* to climate change in Dagangshan forest area of Jiangxi Province. *Chin. J. Appl. Ecol.* 20, 71–76.
- Wang, H.P., Chen, J.H., Zhang, S.D., Zhang, D.D., Wang, Z.L., Xu, Q.H., et al., 2018. A chironomid-based record of temperature variability during the past 4000 years in northern China and its possible societal implications. *Clim. Past* 14, 383–396. <https://doi.org/10.5194/cp-14-383-2018>.
- Wang, Z.J., 1995. Historical investigation of climate change in Qin and Han Dynasties. *Historical Res.* 2, 3–19.
- Wang, J.J., 2007. Research on the Relationship Between Climate Chances and Wars in Chinese Historical. Zhejiang Normal University.

- Wang, S.Z., Fang, Y.M., Zhao, Z.J., 2012. Vegetation, paleoclimate and vegetation use during Longshan case studies of anthracology of Wadian site in Henan Province. *Quat. Sci.* 32, 226–235.
- Von Arx, G., Crivellaro, A., Prendin, A.L., Čufar, K., Carrer, M., 2016. Quantitative wood anatomy-practical guidelines. *Front. Plant Sci.* 7, 781. <https://doi.org/10.3389/fpls.2016.00781>.
- Wiles, G.C., Calkin, P.E., Jacoby, G.C., 1996. Tree-ring analysis and Quaternary geology: principles and recent applications. *Geomorphology* 16, 259–272. [https://doi.org/10.1016/S0169-555X\(96\)80005-5](https://doi.org/10.1016/S0169-555X(96)80005-5).
- Wu, D.Q., Xu, Y.J., Zou, H.B., 1985. An Identification of Ancient Wood Found Han Tomb No.2 at Shennjushan in Gaoyou. *Journal of Nanjing Forestry University (Natural Sciences Edition)* 9, 91–96+145–147.
- Xu, G.B., Broadman, E., Dorado-Liñán, I., Klippel, L., Meko, M., Büntgen, U., et al., 2024. Jet stream controls on European climate and agriculture since 1300 ce. *Nature* 634, 600–608. <https://doi.org/10.1038/s41586-024-07985-x>.
- Xu, R.H., Xie, S.Y., Zhao, Y., 1994. The Holocene environmental evolution and the rise and fall of lakes in the Jianghan Plain. *Areal Res. Dev.* 52–56.
- Yao, S.G., 2013. A brief discussion on flood and drought disasters from Pre-Qin to Qin and Han dynasties. *Agri. Archaeol.* 4, 127–133.
- Yin, Z.Q., Han, Y.B., Ma, L.H., 2021. The possible influence of solar activity and paleoclimate change on the war in Eastern Zhou dynasty. *Astronomical Res. Technol.* 18, 567–575. <https://doi.org/10.14005/j.cnki.issn1672-7673.20210112.001>.
- Zeng, X.Y., 2000. Slices of rotten wood. *Forest sci. technol. Newslett.* 2, 14.
- Zhang, C., Zhao, C., Zhou, A.F., Zhang, H.X., Liu, W.G., Feng, X.P., et al., 2021a. Quantification of temperature and precipitation changes in northern China during the “5000-year” Chinese history. *Quat. Sci. Rev.* 255, 106819. <https://doi.org/10.1016/j.quascirev.2021.106819>.
- Zhang, D., Fang, K.Y., Jia, X., Zhou, F.F., Mei, Z.P., Xiao, Z.C., et al., 2024. Species identification and research potential of dendrochronology to Tang and Song dynasties coffins in northern Jiangsu Province, China. *Quat. Sci.* 44. <https://doi.org/10.11928/j.issn.1001-7410.2024.04.14>.
- Zhang, D., Zhan, Z.Y., Lin, C.S., He, Y.Q., Li, F., 2004. Climate change and war, social unrest and dynastic change in China. *Chin. Sci. Bull.* 23, 2468–2474.
- Zhang, H.W., Cheng, H., Sinha, A., Spötl, C., Cai, Y.J., Liu, B., et al., 2021c. Collapse of the Liangzhu and other Neolithic cultures in the lower Yangtze region in response to climate change. *Sci. Adv.* 7, eabi9275. <https://doi.org/10.1126/sciadv.abi9275>.
- Zhang, J.F., 2020. The Legal System of the Spring and Autumn and Warring States Period Featured by Social Transformation and Legal Reform, the History of Chinese Legal Civilization: Ancient China—From About 21st Century B.C. to 1840 A.D. Springer Singapore, Singapore, pp. 113–156. https://doi.org/10.1007/978-981-10-1029-3_3.
- Zhang, J.J., Zhu, H.B., 2016. Summary of the research on ecological environmental history in the Qin and Han Dynasties. *J. Xianyang Norm. Univ.* 31, 28–34.
- Zhang, W.J., Shi, J.F., Zhao, Y.S., Shi, S.Y., Ma, X.Q., Zhu, Y.X., 2021b. December–March temperature reconstruction from tree-ring earlywood width in southeastern China during the period of 1871–2016. *Int. J. Biometeorol.* 65, 883–894. <https://doi.org/10.1007/s00484-020-02067-9>.
- Zhang, Y.X., Ye, W., Ma, C.M., Li, Y.L., Li, C.H., Zhu, L.D., 2020. Middle to late Holocene changes in climate, hydrology, vegetation and culture on the Hangjiahu Plain, Southeast China. *J. Paleolimnol.* 64, 211–223. <https://doi.org/10.1007/s10933-020-00132-2>.
- Zhang, Z.B., 2007. *Epidemic Chronology of Ancient China*. Fujian Science and Technology Press, Fujian.
- Zheng, J.Y., Xiao, L.B., Fang, X.Q., Hao, Z.X., Ge, Q.S., Li, B.B., 2014. How climate change impacted the collapse of the Ming dynasty. *Clim. Change* 127, 169–182. <https://doi.org/10.1007/s10584-014-1244-7>.
- Zhu, K.Z., 1972. Preliminary study on climate change in China in the past five thousand years. *Acta Archaeol. Sin.* 1, 15–38.
- Zhu, L.S., Hui, Q., Du, P., Chen, Y.M., Du, C., 2022. Excavation of the Eastern Han tomb in Zhangzhuang, Haizhou District, Lianyuangang, Jiangsu. *South. Cult.* 2, 71–84+201–202.
- Zonneveld, K.A.F., Harper, K., Klügel, A., Chen, L., Lange, G.D., Versteegh, G.J.M., 2024. Climate change, society, and pandemic disease in Roman Italy between 200 BCE and 600 CE. *Sci. Adv.* 10, eadk1033. <https://doi.org/10.1126/sciadv.adk1033>.